Effects of superheat degree on flow field of multi-hole fuel sprays

Ming Zhang, Min Xu*, Yuyin Zhang, Wei Zeng
Shanghai Jiao Tong University, Shanghai, China, People's Republic of

ABSTRACT

Superheated spray has the potential to improve the fuel atomization and evaporation processes which is quite attractive for engineering application. However, the mechanism of superheated spray is still not clear yet. In this study, n-hexane sprays from an eight-hole injector in both vertical and cross-sectional planes under various superheat degrees were investigated by using high-speed Particle Image Velocimetry (HS-PIV) technique within the lower density region. In cross-sectional direction, the spray pattern changes from the eight plumes to a "donut" shape, a "pancake" shape and then an "octopus arms" shape as the superheat degree increases. In vertical direction, a lost momentum of spray particles with increased fuel temperature under non-superheated conditions can be observed through the flow field, resulting in a shorter penetration. As the fuel spray enters into the superheated region, significant flash-boiling induced plume expansion with increased superheat degree is observed; the vertical velocity increases while the radial velocity decreases with increasing superheat degree, which results in spray plumes collapsing to the injector axis (gas-jet shape under fully superheated conditions) and dramatically penetration increment under highly superheated conditions. The self-preserving velocity behavior of the gas-jet shape plume is captured and analyzed for fully-superheated sprays (SD>48^{o}C). Obvious vortex at the spray plume outer boundary is observed. The vortex core of fuel sprays is identified. The vortex intensity and the vortex motion under various superheat degrees are also characterized, which are proved to be greatly dependent on the superheat degree. The results provide insight to the spray-collapsing processes under superheated conditions for multi-hole sprays. It's regarded that superheat degree is the predominant factor influencing the flow field, thus the structure of the superheated spray.

INTRODUCTION

To meet the increasing demand for better fuel economy and lower engine emissions, the number of passenger car with spark-ignition direct-injection (SIDI) engines is increasing significantly recently. SIDI technique is expected to improve engine performance dramatically due to more accurate mass control of fuel injection, less cycle-to-cycle variation, higher compression ratio and higher volumetric efficiency, compared to port-fuel injection (PFI) engines [1]. On the other hand, SIDI engines require a higher quality of fuel atomization and evaporation, i.e., smaller dropsize and higher evaporation rate, to achieve desirable fuel-air mixture in a shorter time as the fuel is usually injected directly into cylinders in the late intake stroke or the compression stroke in a SIDI engine. Therefore, to improve the spray quality and to optimize the mixture formation processes is crucial for SIDI engines.

Higher evaporation rate of a fuel spray can be realized by increasing the ratio of total surface area to the total volume of fuel droplets in the spray. The ratio varies with the mean size of droplets in the spray. To obtain a spray with smaller droplet mean diameter, the usual approach is to increase the injection pressure and minimize the injection orifice diameter, which has been investigated for several decades. Hiroyasu and Arai [2] summarized various researches at different conditions of fuel properties, ambient gas pressure, and nozzle configuration. However, the effect of higher injection pressure is limited in improvement of atomization when pressure becomes adequately high, which may lead to such disadvantages as large penetration (thus wall-wetting), oil dilution, piston carbon deposits, worsen emissions, and cost increase of injection system.

In our previous studies [3-6], it's found that much more flexible spray structure and better evaporation become possible when elevating the fuel temperature to make it flash-boiling at the exit of nozzle. The spray structure, the atomization and evaporation characteristics are predominantly influenced by the superheat degree, which depends mostly on the temperature and the vapor pressure of the fuel, the back pressure of ambient gas, and not so sensitive to the injection pressure as the conventional spray. It is also clarified that in the plane containing the spray axis, at low superheat degree (SD) it shows a slight collapsed spray structure with a shorter penetration and a narrower but more uniform spray distribution. Further increasing superheat degree results in a more dramatic spray collapsing and a larger spray penetration. In the cross-sectional plane perpendicular to the spray axis, the spray pattern changes from the eight plumes to a "donut" shape, then a "pancake" shape and an "octopus arms" shape as the superheat degree increases [5]. As for spray evaporation, the vapor concentration is measured through the LIEF technique and turns out to be a function of superheat degree [4]. However, the

* Corresponding author: mxu@sjtu.edu.cn

mechanism of the flash-boiling spray formation which makes the significant difference in characteristics of atomization and evaporation from the conventional spray is not clear.

In this study, the spray flow field was investigated under different fuel temperatures and ambient pressures by means of high-speed Particle Image Velocimetry (PIV). Vortex motion of superheated fuel sprays is identified base on critical point analysis, and the self-preserving velocity behavior under high-superheated conditions is analyzed. The purpose is to characterize the superheated spray flow fields and to understand the transformation process from the conventional spray to the flash-boiling spray as the superheat degree increases.

EXPERIMENT

1. Apparatus

Figure 1 shows the schematic of the experimental apparatus consisting of a constant volume pressure chamber, a fuel supply system, a fluid temperature control system, an ambient gas pressure control system (vacuum pump and pressurized nitrogen gas supply) and a high-speed PIV system.

The pressure chamber has an inner diameter of 203mm and four quartz windows for optical access to the spray. The vacuum system was used to control the chamber ambient pressure as low as 20kPa (absolute pressure). The fuel temperature was controlled through a heat exchanger installed near the nozzle could be regulated between -10 ℃ to 95 ℃ at the injector tip. A hydraulic piston type accumulator was used to pressurize the testing fuel (n-hexane in this work) up to 20.7MPa for the injector.

A high-speed Nd:YLF laser (Litron LDY 300 series, Pulse Width: 170ns, Power: 23.09mJ at 1 kHz) was operated at 527nm. The laser sheets were adjusted to a width of approximately 1.0 mm. The inter-pulse delay time (dt) was set at 10μs. A high-speed Phantom CMOS camera, with a full resolution of 800×600 pixels, was fitted with a Nikon UV lens.

Twenty pairs of spray images were captured at each test condition. The PIV system and the injector were synchronized by using a SRS DG-645 pulse generator and a high-speed controller. The raw PIV image data was analyzed using a multi-pass cross-correlation algorithm to compute the vector fields. MatLab was also used for other data processing.

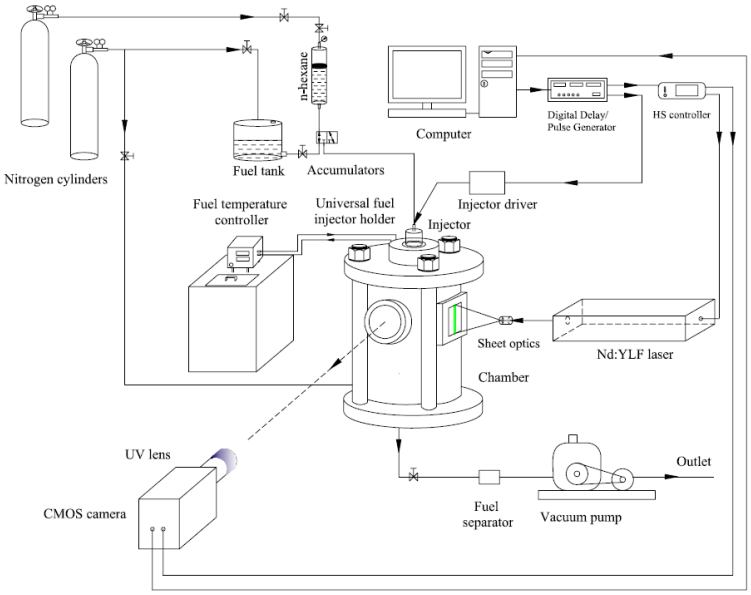

Fig.1 Experimental apparatus

2. Definitions

The fuel superheat degree is defined as the difference between the fuel temperature and the fuel boiling point temperature at the testing ambient pressure, i.e.,

$$SD = T_f - T_{bp.} \qquad (1)$$

The identification and tracking of vortex structures is the key point of this work. There have been numerous studies on techniques for the identification of vortices which involved critical-point analysis of the local velocity gradient tensor and its corresponding eigenvalues. Chone et al. [7] analyzed the eigenvalue characterization of local velocity gradient tensor in three dimensions. To accommodate two dimensional PIV flow field application, Adrian et al. [8, 9] put forward an equivalent form of this tensor as

$$D^{2D} = \begin{bmatrix} \frac{\partial Vx}{\partial x} & \frac{\partial Vx}{\partial y} \\ \frac{\partial Vy}{\partial x} & \frac{\partial Vy}{\partial y} \end{bmatrix} = \begin{bmatrix} E_{xx} & E_{xy} \\ E_{yx} & E_{yy} \end{bmatrix} . \qquad (2)$$

where, E_{ij} is the strain tensor representing the gradient of i^{th} vector component in j^{th} axis (direction). For example,

- $E_{xx} = dV_x/dx$ is the gradient of V_x along x-axis direction and represents compression or expansion;
- $E_{xy} = dV_x/dy$ is the gradient of V_x along the y-axis direction and represents a horizontal shear.

D^{2D} has two real eigenvalues or a pair of complex conjugate eigenvalues. According to the work of Chone [7] and Adrian [8, 9], vortices can be easily identified by plotting iso-regions of $\lambda_{ci} > 0$. The swirling strength (a vortex marker) is thus defined as equation (3). In practice, high level of vortex strength indicates a location around which the streamlines are closed, namely the location of a vortex core. Swirling strength and vortex core for the corresponding velocity field is presented in Fig.2.

$$\text{Swirling strength} = \max\{0, -(E_{xy}E_{yx} - (E_{xx}E_{yy})/2 + (E_{xx}^2 + E_{yy}^2)/4)\} \quad (3)$$

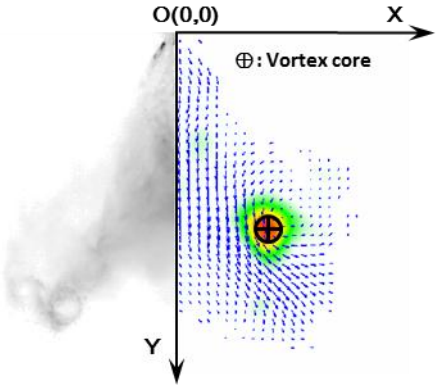

Fig.2 Spray image (left), corresponding flow field and vortex strength distribution (in the right hand side, the red - strong, the yellow - medium, the green - weak)

3. Experimental conditions and testing fuel

N-hexane was chosen for the testing fuel because it is pure substance (easy to determine the superheated level) and one of the substitutes for gasoline for numerical simulation. The experimental conditions are shown in Table 1. The physical properties of n-hexane are listed in Table 2 with comparison to those of gasoline. The ambient pressure (absolute) was varied from 20kPa to 100kPa, which simulates the in-cylinder pressures during intake stroke at different throttling positions in a real SIDI engine. The fuel temperature was varied from 25°C to 90°C, which may occur under a cold start condition and the other warm conditions. Correspondingly, the superheat degree (SD) varies in the range of -43 to 65°C.

Table.1 Experimental conditions

Test fuel	n-hexane (97%)
Injection pressure (MPa)	5
Ambient temperature (℃)	25±1
Fuel temperature, T_f (℃)	25~90
Ambient pressure (kPa)	20~100
Injection pulse width (μs)	1000

Table.2 Physical properties of n-hexane (25 ℃)

	Viscosity (mPa s)	Density (g/mL)	Surface tension (mN/m)
n-hexane	0.292	0.759	18.4
Gasoline	0.42	0.74	20-25

RESULTS AND DISCUSSIONS

1. Axial spray structure and cross-sectional spray pattern

Figure 3 shows the typical spray images under various superheated conditions in both vertical (in the plane through the spray axis) and cross-sectional (10/20/30 mm downstream the nozzle tip) directions. A significant transformation in the spray structure in both directions can be observed by comparing these images. Under non-superheated conditions (T_{fuel}=25ºC, SD=-17ºC), the eight individual plumes (each denoted by a small circular speckle) are evenly distributed on cross-sectional planes (Fig. 3(a)). However, when the fuel is heated to 60°C (Fig. 3(b)), there appears remarkable spray deformation. Specifically, each plume expands around its center and centers of all eight plumes move toward the spray axis. From the view of vertical plane, it can be found obvious-

ly that spray plumes start to connect and interact with each other, and that both the penetration and the width between the adjacent plumes shrinks dramatically. At the fuel temperature of 80°C (Fig. 3(c)), the original eight plumes join together completely and form a "pancake" shape structure that the boundary of original eight spray plumes is indistinct. A compact bell-shape structure is observed in the vertical direction. As the fuel temperature further increased to 90°C (Fig. 3(d)), the cross-sectional spray structure changes to a pancake shape with eight "octopus arms". In vertical direction, a gas-jet-like spray structure can be observed and the spray width becomes quite narrow; an extended spray tip travelling ahead of main spray body can be seen near the centerline, which results in a significant increase in the re-surged penetration. A detail schematic illustration of the transformation process of the cross-sectional spray pattern as a function of the superheat degree can be referred to [5].

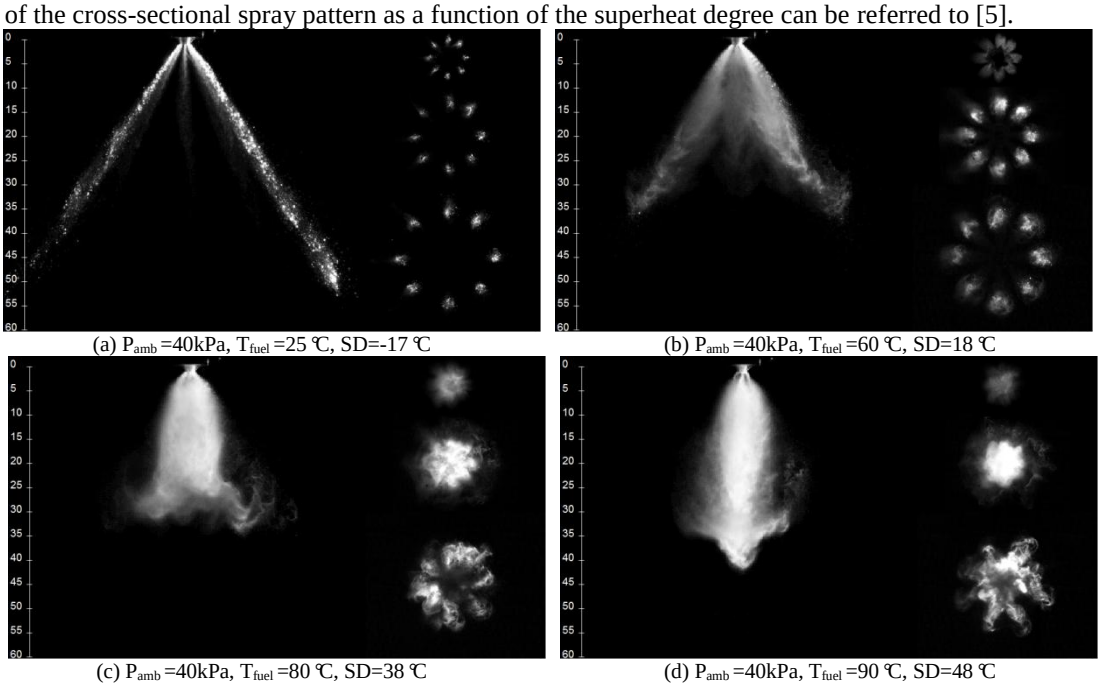

(a) P_{amb} =40kPa, T_{fuel} =25 ℃, SD=-17 ℃ (b) P_{amb} =40kPa, T_{fuel} =60 ℃, SD=18 ℃

(c) P_{amb} =40kPa, T_{fuel} =80 ℃, SD=38 ℃ (d) P_{amb} =40kPa, T_{fuel} =90 ℃, SD=48 ℃

Fig.3 Spray structures in the axial and the cross-sectional planes under various SD (P_{inj}= 5MPa, t=0.8 ms ASOI)

2. Velocity vector distributions

Figure 4 shows spray velocity vector fields at a fixed ambient pressure of 40kPa and various superheat degrees. At superheat degree of 18 ℃, two main flow streams can be identified, with most velocity vector goes along the designed orifice orientation. The maximum velocity is around 55m/s, locating near each plume tip. When superheat degree increases to 28 ℃, mild collapsed structure is observed; the adjacent spray plumes start to approach and their edges start to interact with each other. The maximum velocity increases slightly compared to the previous condition. When the superheat degree increases to 38 ℃, the maximum velocity keeps increasing and the location of the peak moves toward the spray axis, indicating a collapse effect between spray plumes. Further increasing the superheat degree to 48 ℃, a dramatically increased velocity higher than 70m/s can be seen near the spray centerline; the peak location keeps moving down along the centerline.

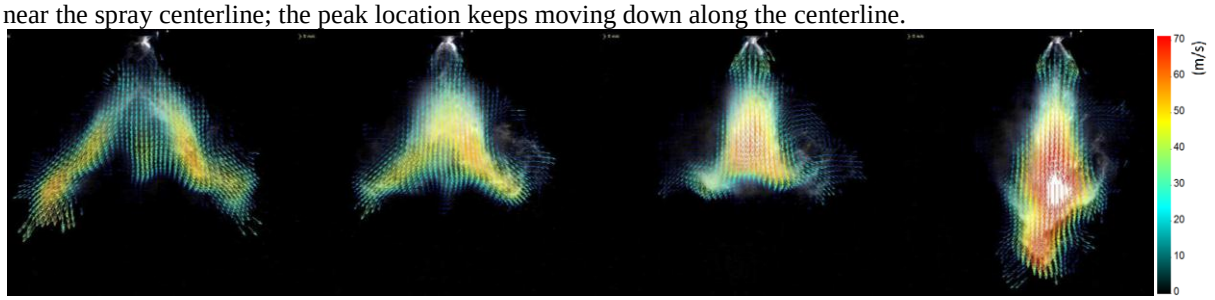

P_{amb} =40kPa, T_{fuel} =60 ℃ SD=18 ℃ | P_{amb} =40kPa, T_{fuel} =70 ℃ SD=28 ℃ | P_{amb} =40kPa, T_{fuel} =80 ℃ SD=38 ℃ | P_{amb} =40kPa, T_{fuel} =90 ℃ SD=48 ℃

Fig.4 Velocity vectors of fuel spray under various superheated degree (t=1.0ms ASOI, P_{amb}=40kPa)

The Y-component (Y is the spray centerline direction) of the velocity vectors at four planes (10/20/30/40mm) downstream the nozzle tip are shown in Fig. 5. At superheat degree lower than 30 ℃, an overwhelming bimodal velocity distributions can be observed in Fig.5 (a) and (b), although the noise signal (especially at 20/30mm planes), introduced by plumes other than the two examined plumes, can be found in (a). When superheat degree exceeds 38 ℃ (Fig.5 (c) and (d)), unimodal velocity distributions appear instead of bimodal velocity distribution, indicating the plumes begin to collapse into one. The collapse effect results in a conspicuous increment of y-component velocity, compared to the profiles with cases with lower superheat degrees in Fig.5 (a) and (b). How-

ever, the increment is not so significant until the superheat degree increase to 48 ℃ that this unimodal vector distribution shows a characteristic of self-preserving jet as shown in (d). In the same Fig.5 (d), a dramatic increment of y-component velocity due to the same collapse effect and an insignificant velocity drop after the velocity peak can be seen by comparing the profile at 30mm and 40mm.

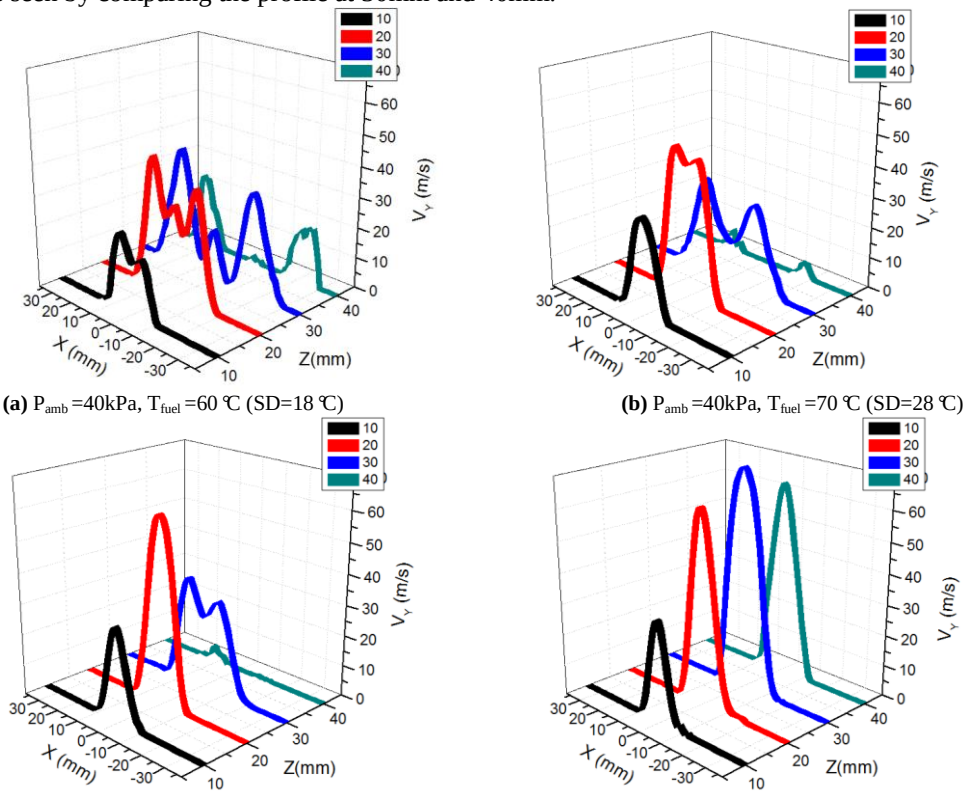

(a) P_{amb} =40kPa, T_{fuel} =60 ℃ (SD=18 ℃) **(b)** P_{amb} =40kPa, T_{fuel} =70 ℃ (SD=28 ℃)

(c) P_{amb} =40kPa, T_{fuel} =80 ℃ (SD=38 ℃) **(d)** P_{amb} =40kPa, T_{fuel} =90 ℃ (SD=48 ℃)

Fig.5 Profiles of Y-component velocity at 10(black) /20(red) /30(blue) /40(green) mm downstream the nozzle under various superheat degrees

3. Self-preserving flow structure under high superheated conditions

The self-preserving flow structure of fuel spray under fully superheated conditions **(**P_{amb} =40kPa, T_{fuel} =90 ℃, SD=48 ℃) will be examined in this section. In Fig.6, the y-component velocity was normalized by the maximum velocity at each plane, i.e., V_y/V_{ymax}, and the radial distance is normalized by the radial distance where the velocity is 0.5*V_{ymax} ($X/X_{Vy=0.5Vymax}$). The profiles cover a wide range from about 11mm downstream the nozzle tip to the location near the spray tip.

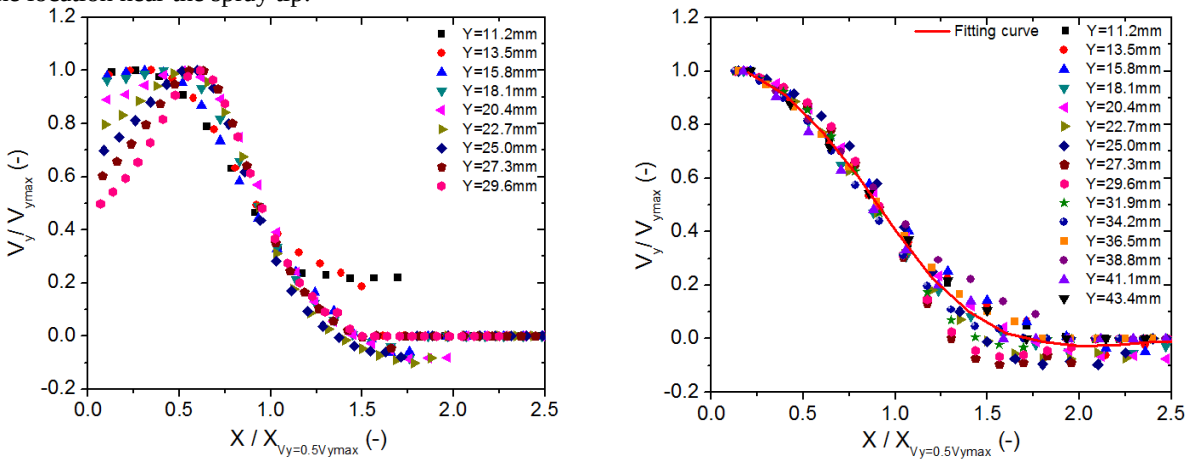

(a) P_{amb} =40kPa, T_{fuel} =70 ℃ (SD=28 ℃) **(b)** P_{amb} =40kPa, T_{fuel} =90 ℃ (SD=48 ℃)

Fig.6 Profiles of normalized Y-component velocity under various superheat degrees (t=1.0ms ASOI)

The normalized velocity profiles (Y-component) in two flash-boiling sprays are shown in Fig. 6(a) (SD=28 ℃) and Fig. 6(b) (SD=48 ℃), at different axial distance from the nozzle tip. For the case of SD=28 ℃, Fig. 6(a), there appears only peak near the centerline of the spray at the near-nozzle-tip region, but two peaks at the near-spray-tip region. For the case of SD=48 ℃, Fig. 6(b), the dots lie on or close to a fitting curve which has only one peak. The fitting curve is quite similar to that of the single gas jet measured by Gutmark [10], alt-

hough the results near the spray boundary ($X/X_{Vy=0.5Vymax}$>1.25) do not conform right to the fitting curve owing to the strong interaction between liquid droplets in the spray and the surrounding gas. In addition to the velocity distributions, this gas-jet characteristic of the fully superheated fuel spray has also been confirmed by the previous fuel liquid/vapor distribution measurements based on Laser Induced Exciplex Fluorescence (LIEF) technique [4]. The vapor phase concentrates itself near the centerline and forms a flow like a gas jet injected from the nozzle holes when increasing superheat degree to a high level (here, SD=50 ℃), while the liquid droplets scatters around the spray as shown in Fig. 7.

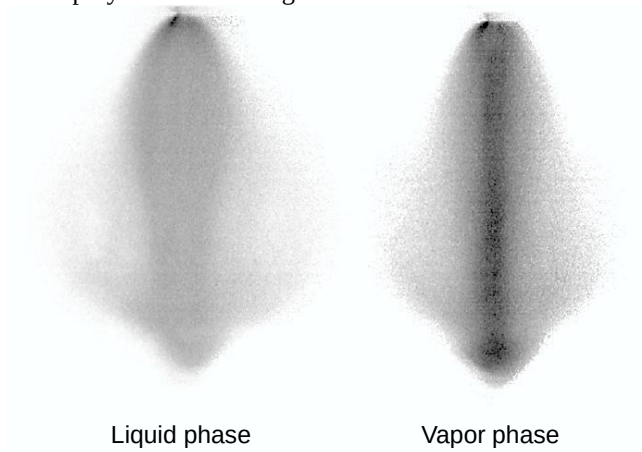

Fig.7 Liquid and vapor distributions of n-hexane spray from the same multi-hole injector (SD=50 ℃) [4]

4. Vortex core movement and swirling strength

The vortex core identification and swirling strength comparison are performed here to investigate their relation to the superheat degree and their effects on the flow field and corresponding spray structure.

The velocity vector distribution comparison between case SD=29 ℃ and case SD=37 ℃ is shown in the first and the second rows respectively in Fig.8. At 1.0ms ASOI, both cases show bell-shaped collapsed spray structure but case SD=37 ℃ has slightly larger velocity magnitude. As the time elapses, an opposite trend of the vortex core appears for the two cases. A predominant radially-stretched flow structure is captured in case SD=29 ℃ as the vortex core moves outward but the penetration almost keeps constant. In case of SD=37 ℃, stronger y-component velocity near the spray centerline and the vortex core moves inwardly to the injector axis can be observed, implying that the fuel plumes collapse toward the centerline at a higher SD condition is caused by the vortex movement.

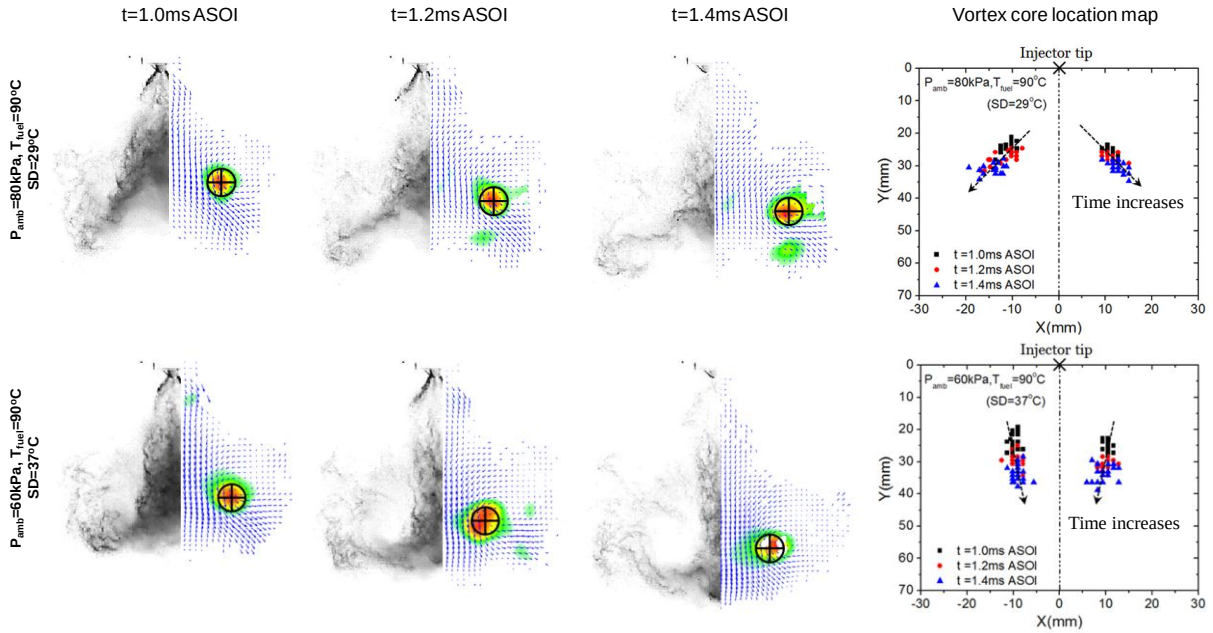

Fig.8 Spray structure, flow fields and corresponding vortex core movement under SD=29 ℃ and 37 ℃

The trend of the vortex core movement in the flash-boiling spray at 1.0ms ASOI is shown in Fig.9 under various superheat degrees by either (a) adjusting the fuel temperature at fixed ambient pressure of 40kPa or, (b) adjusting the ambient pressure at a fixed fuel temperature of 90 ℃. In the both cases, the vortex core move towards the injector axis in the radial direction and moves downwards in the axial direction as superheat degree

increases, indicating that the superheat degree is the predominant parameter for the vortex core movement and, a higher superheat degree causes a stronger tendency of the vortex core movement toward the spray centerline.

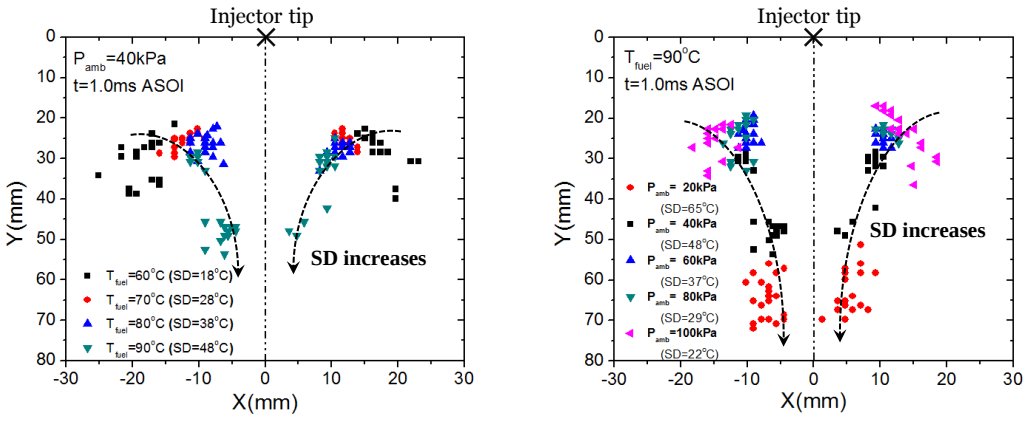

(a) By adjusting fuel temperature (b) By adjusting ambient pressure

Fig. 9 Vortex core under various superheat degrees (t=1.0ms ASOI)

The 20-cycles-averaged swirling strength at the vortex core under various superheat degrees is compared in Fig.10. The strength increases monotonically with the superheat degrees either by adjusting the fuel temperature (solid line) or the ambient pressure (dash line). Thus it's concluded by combining the data in Fig.9 and 10 that the swirling motion is highly dependent on the superheat degree and that either way of adjusting superheat degree plays similar role in affecting the swirling motion and intensity investigated. This increase in the vortex intensity is most likely caused by the vortex core movement toward the centerline as the superheat degree increases, according to the momentum conservation law.

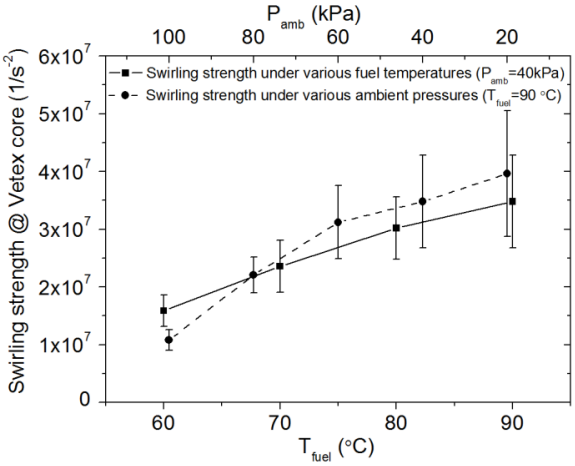

Fig.10 Swirling strength at vortex core under various superheat degrees (t=1.0ms ASOI)

CONCLUSIONS

In this study, the fuel spray structures and the flow fields in axial and cross-sectional directions under superheated conditions are characterized by means of high-speed PIV technique. The effects of superheat degree on the spray structure and flow fields are examined and, the characteristics of the flow fields and the transformation process from the conventional spray to the flash-boiling spray were clarified as the superheat degree increases. The main conclusions are as follows:

(1) An overwhelming bimodal velocity vector distribution is dominant for sprays under low superheated conditions. However, under high superheated conditions, a unimodal velocity vector distribution appears, indicating that the plumes in the spray collapses into one at high superheat degrees and, the spray structure can be controlled easily through fuel temperature as well as the ambient pressure.

(2) Under high superheat degree conditions, the profiles of y-component velocity in a fully flash-boiling spray indicate a conspicuous self-preserving characteristic like in a single gas-jet, which is consistent with the observation through the fuel vapor concentration distributions based on LIEF technique.

(3) An outwardly-moving vortex core results in predominant radial-stretching spray structure under lower superheated conditions. As the superheat degree increases, the collapse effect induced by inwardly-moving vortex core leads to the fuel spray collapsing to the spray centerline. A higher superheat degree causes a

stronger tendency of the vortex core movement toward the spray centerline.

(4) The vortex core location and the vortex intensity in the superheated fuel spray show strong dependence on the superheat degree, despite of by adjusting the fuel temperature at fixed ambient pressure or by adjusting the ambient pressure at fixed fuel temperature. The vortex core move toward the spray centerline and thus probably causing the vertex intensity to increase when increasing superheat degree.

ACKNOWLEGEMENT

The research was carried out at National Engineering Laboratory for Automotive Electronic Control Technology in Shanghai Jiao Tong University. It is sponsored by National Natural Science Foundation of China grant number 51076090 and Shanghai Pujiang Program grant number 10PJ1406200.

REFERENCES

[1] F. Q. Zhao, M. C. Lai, D. L. Harrington, "Automotive spark-ignited direct-injection gasoline engines," Progress in Energy and Combustion Science, 25: 437–562, 1999.

[2] H. Hiroyasu, M. Arai, "Structure of Fuel Sprays in Diesel Engines," SAE Paper 900475, 1990.

[3] W. Zeng, M. Xu, M. Zhang, Y. Y. Zhang, D. J. Cleary, "Characterization of Methanol and Ethanol Sprays from Different DI Injectors by Using Mie-Scattering and Laser Induced Fluorescence at Potential Engine Cold-Start Conditions," SAE Paper 2010-01-0602, 2010.

[4] G. M. Zhang, M. Xu, Y. Y. Zhang, W. Zeng, "Quantitative Measurements of Liquid and Vapor Distributions in Flash Boiling Fuel Sprays using Planar Laser Induced Exciplex Technique," SAE Paper 2011-01-1879, 2011.

[5] M. Zhang, M. Xu, Y. Y. Zhang, W. Zeng, "Flow-field Evaluation of Superheated Fuel Sprays using High-speed PIV," SAE Paper 2011-01-1880, 2011.

[6] M. Zhang, M. Xu, Y. Y. Zhang, W. Zeng, "Flow Field Characterization of Superheated Sprays from a Multi-hole Injector by Using High-speed PIV," SAE Paper 2012-01-0457, 2012.

[7] M. S. Chone, A. E. Perrey, Cantwell BJ, "A general classification of three-dimensional flow fields," Phys. Fluids A2 (1990): 765-777, 1990.

[8] R. J. Adrian, K. T. Christensen, Liu ZC, "Analysis and interpretation of instantaneous turbulent velocity fields," Exp. in Fluids (2000), 29/3, pp. 275-290, 2000.

[9] J. Zhou, R. J. Adrian et al., "Mechanisms for generating coherent packets of hairpin vortices in channel flow," J. Fluid Mech. (1999), vol.387, pp. 353-396, 1999.

[10] E. Gutmark, I. Wygnaski, "The planar turbulent jets," J. J. Fluid Mech. (1976) vol.73, pp. 465-495, 1976.